J. Mol. Biol. (1995) **248**, 824–834

JMB

Structural Model of the Phospholamban Ion Channel Complex in Phospholipid Membranes

Isaiah T. Arkin[1], Matthew Rothman[3], Cheryl F. C. Ludlam[3] Saburo Aimoto[4], Donald M. Engelman[2], Kenneth J. Rothschild[3] and Steven O. Smith[2]*

[1]*Department of Cell Biology Yale University School of Medicine, New Haven CT 06510, U.S.A.*

[2]*Department of Molecular Biophysics & Biochemistry Yale University, Box 208114 New Haven, CT, 06520 U.S.A.*

[3]*Department of Physics and Molecular Biophysics Laboratory, Boston University, Boston MA 02215, U.S.A.*

[4]*Institute for Protein Research, Osaka University Osaka 565, Japan*

**Corresponding author*

Phospholamban is a 52 amino acid residue membrane protein involved with the regulation of calcium levels across sarcoplasmic reticulum membranes in cardiac muscle cells. The N-terminal 30 amino acid residues of the protein are largely hydrophilic and include two sites whose phosphorylation is thought to dissociate an inhibitory complex between phospholamban and Ca^{2+} ATPase. The C-terminal 22 amino acid residues are largely hydrophobic, anchor the protein in the membrane and are responsible for Ca^{2+} selective ion conductance. Specific interactions between the transmembrane domains stabilize a pentameric protein complex. We have obtained circular dichroism (CD), transmission Fourier transform infrared (FTIR) and attenuated total reflection Fourier transform infrared (ATR-FTIR) spectra of the full-length protein and have compared these results to those from a 28 residue peptide that includes the transmembrane domain. Both proteins reconstituted into phospholipid membranes are largely α-helical by CD and FTIR. Polarized ATR-FTIR measurements show that both the cytosolic and transmembrane helices are oriented perpendicular to the membrane plane with a tilt of $28(\pm 6)°$ with respect to the membrane normal. This tilt angle is in close agreement to that calculated from a model for the transmembrane domain of phospholamban suggested by mutagenesis and molecular modeling. Phosphorylation does not significantly change the secondary structure or orientation of the protein. The pentameric complex is modeled as a left-handed coiled-coil of five long helices ($40(\pm 3)$ residues) that extend across the membrane from the lumenal carboxy terminus to the phosphorylation site in the cytoplasm. The helix bundle forms a perpendicular ion pore that may begin at a distance (17 to 29 Å) from the membrane surface. Based on the above, we propose a mechanism by which phospholamban regulates Ca^{2+} levels across membranes that takes into account both its selective ion conductance and inhibitory association with the Ca^{2+} pump.

Keywords: membrane protein; ATR-FTIR; secondary structure; sarcoplasmic reticulum; Ca^{2+} regulation

Introduction

In the past decade, amino acid sequences have been determined for many of the physiologically important mammalian ion channels. A common structural motif suggested by sequence analysis is that these proteins span cell membranes with hydrophobic helices and that bundles of helices form ion-conducting pores (Catterall, 1991). These proteins are generally composed of repeating subunits either as oligomers (e.g. the K^+ channels) or as homologous domains in a single protein that

Abbreviations used: ATR, attenuated total reflection; FTIR, Fourier transform infrared; FSD, Fourier self-deconvolution; CD, circular dichroism; DMPC, 1,2-dimyristoyl phosphatidylcholine; PLBWT, wild-type full-length human phospholamban; PLBWT-P, phosphorylated (Ser16) wild-type full-length human phospholamban; PLBTM, a synthetic peptide corresponding to residues 25 to 52 of human phospholamban that contains the transmembrane domain; SR, sarcoplasmic reticulum; TM, transmembrane; RP-HPLC, reverse phase high performance liquid chromatography.

0022–2836/95/190824–11 $08.00/0

presumably arose from gene duplication (e.g. Ca^{2+} and Na^{+} channels (Catterall, 1991)). A low resolution structure of the acetylcholine receptor has suggested a bundle of five helices in the core of the receptor complex that define a central ion channel (Unwin, 1993). The size and complexity of most ion channels, however, has prevented high resolution structural studies capable of addressing how these proteins are regulated in terms of their gating and ion specificity.

Phospholamban is a small (52 residues) type II membrane protein found in cardiac sarcoplasmic reticulum (SR). It shares many of the characteristics of the larger mammalian ion channels (Tada *et al*., 1989; Tada, 1992). Most notably, it forms a defined oligomeric structure as observed by SDS-PAGE (Gasser *et al*., 1986; Wegener & Jones, 1984) and exhibits ion selective (Ca^{2+}) single channel conductances (Kovacs *et al*., 1988; Arkin *et al*., 1993). The protein plays a role in the regulation of Ca^{2+} levels across the SR membrane and thus in the contraction / relaxation cycle of cardiac muscle. It is not clear whether the regulation of Ca^{2+} levels by phospholamban involves both passive ion conductance and the regulation of the resident Ca^{2+} pump (James *et al*., 1989). Phospholamban inhibits the steady state activity of the Ca^{2+} pump at submicromolar Ca^{2+} concentrations, while phosphorylation by protein kinases, as a response to β-adrenergic stimulation, relieves this inhibition (Tada & Kadoma, 1989). The small size of the phospholamban channel protein makes it a tractable system for detailed structural studies.

The human phospholamban sequence is comprised of an N-terminal stretch of ~30 hydrophilic residues and a C-terminal stretch of 22 hydrophobic residues corresponding to the transmembrane domain of the protein:

```
      1               5
Ac-NH-Met-Glu-Lys-Val-Gln-Tyr-Leu-Thr
         10                  15  16
      Arg-Ser-Ala-Ile-Arg-Arg-Ala-Ser
                 20
      Thr-Ile-Glu-Met-Pro-Gln-Gln-Ala
      25                  30  31
      Arg-Gln-Lys-Leu-Gln-Asn-Leu-Phe
             35                   40
      Ile-Asn-Phe-Cys-Leu-Ile-Leu-Ile
                      45  46
      Cys-Leu-Leu-Leu-Ile-Cys-Ile-Ile
         50      52
      Val-Met-Leu-Leu-COOH
```

The soluble N-terminal segment extends into the cytosol and contains the sites of phosphorylation at Ser16 and Thr17 (Wegener *et al*., 1989). This segment carries a net +4 charge that may be important in electrostatic interactions at the membrane surface. The C-terminal segment of phospholamban spans membrane bilayers, and interactions between transmembrane (TM) helices stabilize a pentameric complex (Gasser *et al*., 1986; Wegener & Jones, 1984). Recently, mutagenesis (Arkin *et al*., 1994) and molecular modeling (Adams *et al*., 1995) studies performed on the transmembrane domain of phospholamban have suggested which residues lie in the helix interface and / or line the ion pore.

Previous circular dichroism (CD) measurements of detergent-solubilized phospholamban argued that the protein was predominantly helical, but with substantial β-sheet structure (Simmerman *et al*., 1989). In related work (C.F.C.L., I.T.A., X. Liu, S.O.S., D.M.E., S.A. & K.J.R., unpublished results), we showed by Fourier transform infrared (FTIR) studies that the C-terminal segment of phospholamban (PLBTM) is predominantly helical and is protected from $^{1}H/^{2}H$ exchange due to partitioning in the bilayer. However, the structure of the full-length protein in membranes, its native environment, remains an open question. Here, we determine the secondary structure and orientation of phospholamban in phospholipid bilayers. Comparisons between spectroscopic measurements of the full-length wild-type protein (PLBWT) and phosphorylated full-length protein (PLBWT-P) with those of a peptide corresponding to residues 25 to 52, which includes the transmembrane domain (PLBTM), allow us to generate a low resolution structural model of the pentameric channel complex.

Results and Discussion

Secondary structure of PLBWT and PLBTM from CD

The shape and intensity of the CD spectrum between 180 and 240 nm is extremely sensitive to protein secondary structure. For soluble proteins, CD spectra are typically analyzed by deconvolution using a basis set of spectra corresponding to α-helix, β-sheet, β-turn and random coil. The basis CD spectrum for an α-helix exhibits characteristic minima at 208 and 222 nm with magnitudes of $-36{,}000(\pm 3000)$ deg.cm^2 dmol^{-1} and a maximum at 190 to 195 nm with a magnitude of $70{,}000(\pm 10{,}000)$ deg.cm^2 dmol^{-1} (Tinoco *et al*., 1963; Chen *et al*., 1974). Analysis of the CD spectra of membrane proteins is also often done by deconvolution, although it is complicated by differential light scattering and absorption flattening (Duysens, 1956; Long & Urry, 1981; Mao & Wallace, 1984; Park *et al*., 1992). The shape of the CD bands, however, provides a qualitative indication of the secondary structure. The CD spectrum of PLBWT reconstituted into 1,2-dimyristoyl phosphatidylcholine (DMPC) vesicles is shown in Figure 1(a). The spectrum exhibits minima at ~210 nm and 225 nm, and a maximum at 194 nm characteristic of α-helical proteins.

In order to estimate the thermal stability of the protein, a thermal ellipticity profile was obtained by monitoring the CD intensity at 222 nm (Figure 1 (b)). The magnitude of ellipticity does not decrease with

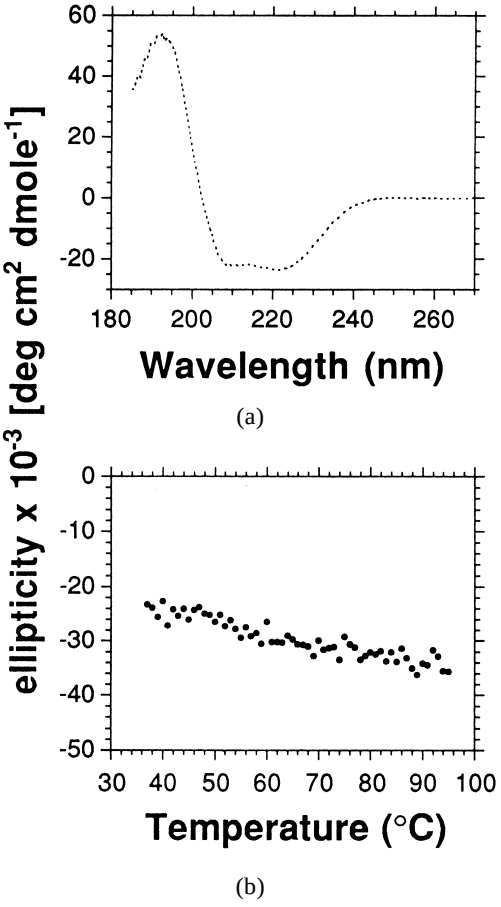

Figure 1. (a) CD spectrum of PLBWT in DMPC vesicles scaled to mean residue ellipticity. The spectrum was obtained at 37°C in 0.2 mM Tris-HCl (pH 7.4). (b) Ellipticity thermal profile of PLBWT at 222 nm.

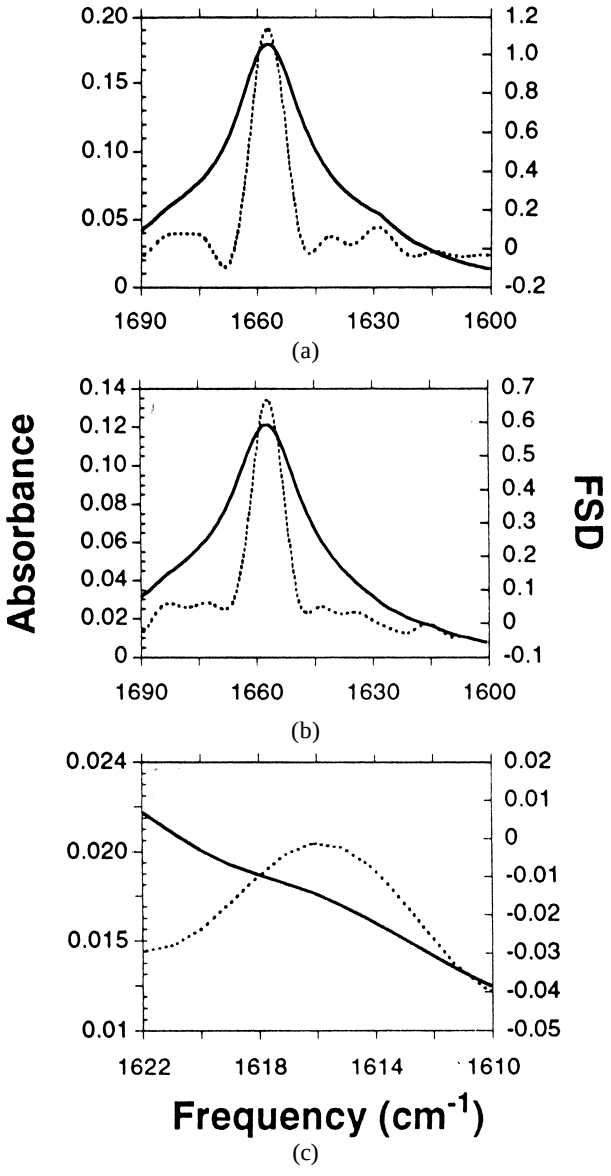

Figure 2. Transmission FTIR spectra and Fourier self-deconvolutions of PLBTM and PLBWT. The transmission FTIR spectra of PLBTM (a) and PLBWT (b) are drawn in continuous lines, while Fourier self-deconvolutions are drawn in broken lines. (c) An expansion of the region of the spectrum of PLBWT that includes the ^{13}C isotope-shifted band. The Fourier self-deconvolutions were obtained with a bandwidth of 13 cm^{-1} and an enhancement factor of 2.4 (see Materials and Methods).

temperature. This clearly indicates that the α-helical content of the protein is not reduced with increased temperature (thermal melting).

Secondary structure of PLBWT and PLBTM from FTIR

As a more definitive measure of secondary structure, we have analyzed transmission FTIR spectra of PLBWT and PLBTM (Figure 2) using Fourier self deconvolution. The frequency of the amide I vibration, due primarily to the C═O stretch, is sensitive to protein secondary structure (Braiman & Rothschild, 1988). Bands centered at ~1654 cm^{-1} correspond to α-helical structures, while bands centered at 1624 to 1637 cm^{-1} and 1675 cm^{-1} correspond to the out-of-phase and in-phase modes of β-sheet structures, respectively (Byler & Susi, 1986), or alternatively to β-turns (Bandekar & Krimm, 1979). The amide I bands for both PLBWT and PLBTM are centered at 1656 cm^{-1} and have highly symmetrical Lorentzian shapes suggesting a high helical content. Furthermore, the relatively narrow band width and absence of hydrogen/deuterium exchange (Susi *et al.*, 1967) rules out the possibility of a random coil structure.

Integration of Fourier self-deconvoluted spectra (Kauppinen *et al.*, 1981) can yield quantitative estimates of the relative ratios between the different secondary structural elements of the protein (Byler & Susi, 1986). Areas of the integrated Fourier self-deconvoluted bands as well as the ratio of the strong 1656 cm^{-1} band to the total intensity in the amide I region from 1600 to 1700 cm^{-1} are listed in Table 1. This analysis does not take into account contributions from side-chain modes (the amido, amino and

Table 1

Amide I intensities and helical percentages for PLBWT and PLBTM

	1616 cm^{-1}		1656 cm^{-1}	
Sample	Intensity[a]	Helical residues / total residues[b]	Intensity[a]	Helical residues / total residues[c]
PLBWT	0.019	0.98 / 52	0.65	40 / 52
PLBTM	0.006	0.17 / 28	0.67	22 / 28

[a] The integrated intensities of the 1616 cm^{-1} and 1656 cm^{-1} bands were determined from the Fourier self-deconvoluted (FSD: see Materials and Methods) FTIR spectra of PLBTM and PLBWT and scaled relative to the intensity of the entire amide I band from 1600 to 1700 cm^{-1}, which was normalized to a value of 1.0.

[b] The number of helical residues represented by the 1616 cm^{-1} band is calculated by dividing the integrated intensity of the 1616 cm^{-1} band determined from FSD spectra by the integrated intensity of the entire amide I region from 1600 to 1700 cm^{-1} and normalizing to the total number of residues in PLBWT (52) or PLBTM (28). The ratios do not account for possible intensity contributions from underlying side-chain vibrations.

[c] The number of helical residues represented by the 1656 cm^{-1} band is calculated by taking the ratio of amide I intensity at 1656 cm^{-1} to the entire amide I intensity and normalizing to the total number of residues in PLBWT (52) or PLBTM (28). For this calculation, we accounted for the differences in extinction coefficients of the different secondary structure elements and the intensities of the various side-chain vibrations (calculated on the basis of the peptide sequence) in the 1600 to 1700 cm^{-1} region of the IR spectrum (Venyaminov & Kalnin 1990*c*); see the text for details.

guanidino side-chains of Gln, Asn, Arg and Lys) that overlap the amide I region. As a result, the helical percentages (0.67 and 0.65 for PLBTM and PLBWT, respectively) determined from the ratio of the peak areas are underestimated. Furthermore, the extinction coefficients for the amide I modes that originate from different secondary structures are not necessarily equal. A recent analytical approach developed by Venyaminov & Kalnin (1990*a*,*b*,*c*) accounts for both of these factors, resulting in estimates of α-helical content of 79% for PLBTM (22($\pm$2) out of 28 residues) and 77% for PLBWT (40($\pm$3) out of 52 residues). Error estimates are derived from the upper and lower limits of the extinction coefficients of side-chain and amide I modes.

The observed amide I bands provide information on the global protein secondary structure. We have recently shown that local secondary structure in a membrane protein can be determined by isotope-induced shifts of the amide I bands (C.F.C.L., I.T.A., X. Liu, S.O.S., D.M.E., S.A. & K.J.R., unpublished results). Incorporation of ^{13}C into the backbone carbonyl group causes a shift of $\sim$40 cm^{-1} in the amide I vibration due to the increased mass (Tadesse *et al*., 1991). Utilizing this approach, PLBWT was specifically ^{13}C labeled at the backbone carbonyl group of Ile12. We observe an increase of intensity at 1616 cm^{-1} that is attributed to a –40 cm^{-1} shift of a component of the strong 1656 cm^{-1} amide I band. The ratio of the 1616 cm^{-1} intensity to that of the total amide I intensity corresponds roughly to 1 amino acid residue out of 52 (Table 1), as expected. For comparison, the intensity of the 1616 cm^{-1} band in unlabeled PLBTM is only $\sim$1% of the 1656 cm^{-1} band, which may be due to the 1.1% natural abundance of ^{13}C. These results establish that Ile12 is in a helical geometry. Furthermore, after establishing that residue Ile12 is in a helical part of the protein, residue $i + 4$ (Ser16) must also be in a helical geometry (as are the intervening residues Arg13 to Ala15) since it contributes the proton in the hydrogen bonding scheme of an α-helix.

Orientation of PLBWT and PLBTM

The CD and FTIR results establish that the cytosolic N-terminal and hydrophobic C-terminal segments of the protein are largely helical. The length of the membrane segment ($\sim$22 amino acid residues) suggests that the C-terminal helix spans the bilayer in an orientation perpendicular to the membrane plane. The intriguing question at this stage regards the orientation of the cytosolic helix.

Polarized attenuated total reflection (ATR)-FTIR can be used to determine the relative orientation of α-helices in oriented membranes by measuring the dichroism of the Fourier self-deconvoluted α-helical amide I vibrational mode. Figure 3 presents ATR-FTIR spectra of both PLBWT and PLBTM obtained with parallel and perpendicular polarized light along with their corresponding Fourier self-deconvolutions. Table 2 lists the measured dichroic ratios, derived order parameters and corresponding tilt angles (see below) for PLBWT and PLBTM. In these measurements, the lipid vibrations serve as internal standards for estimating the overall orientation of the membranes. The average order parameter ($S_{\text{lipid CH2}} = 0.72$) obtained for the lipid

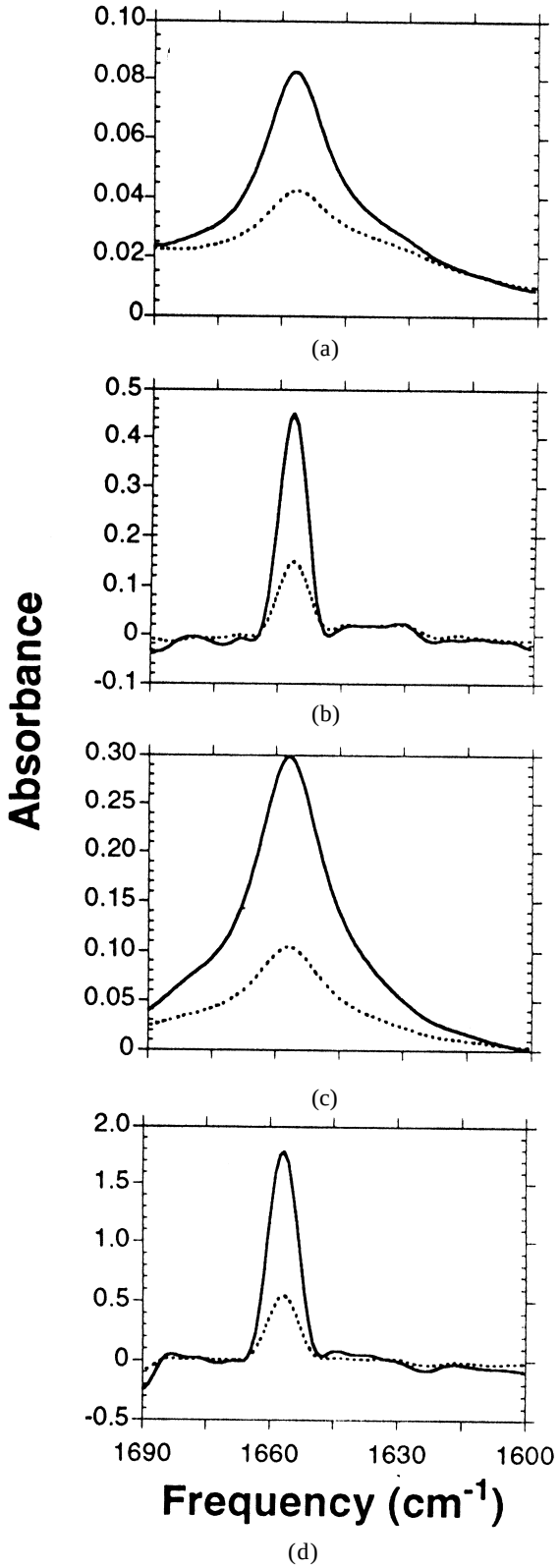

Figure 3. Polarized ATR-FTlR spectra and Fourier self-deconvolutions of PLBTM and PLBWT. The polarized ATR-FTIR spectra of PLBTM (a) and PLBWT (c) were obtained using parallel (continuous line) or perpendicular (broken line) polarized light. The Fourier self-deconvolutions of PLBTM (b) and PLBWT (d) were obtained with a bandwidth of 13 cm^{-1} and an enhancement factor of 2.4 (see Materials and Methods).

methylene symmetric (2852 cm^{-1}) and asymmetric (2924 cm^{-1}) stretching modes indicates that the membranes are reasonably well-oriented (Smith *et al*., 1994). We can define an order parameter for overall membrane orientation ($S_{membrane}$ = 0.76) based on the lipid order parameter by accounting for a 10° tilt of the lipid acyl chains in gel phase membranes (Hauser *et al*., 1981).

Limits on the maximum helix tilt angle relative to the membrane normal can be determined from the maximum dichroic ratios and corresponding helix order parameters for PLBWT (R^{ATR} = 3.31, S_{helix} = 0.54) and PLBTM (R^{ATR} = 3.43, S_{helix} = 0.58). The maximum observed dichroic ratios correspond to those observed for the most well-ordered proteins and translate into tilt angles for PLBTM and PLBWT of 32° and 34°, respectively. These values are obtained by assuming that the membranes are perfectly oriented ($S_{membrane}$ = 1.0) parallel to the surface of the internal reflection element and that the ''low'' helix order parameters result entirely from a tilt away from the bilayer normal. In a similar fashion, limits on the minimum helix tilt angles can be determined by considering the membrane orientation and assuming that the ''low'' helix order parameters result from a combination of helix tilt and membrane disorder. In this case, the helix order parameters are increased by a factor ($1/S_{membrane}$ = 1.32), which accounts for disorder in membrane orientation. The minimum tilt angles for PLBTM and PLBWT derived in this manner are 23° and 26°, respectively. Taken together, the minimum and maximum limits define the range of possible helix tilt angles for PLBTM ($\theta = 27.5(\pm 4.5)°$) and PLBWT ($\theta = 30\ (\pm 4)°$). These values are in approximate agreement with the tilt angle ($\theta = 23°$) that can be calculated from the model we have derived from mutagenesis and molecular modeling studies of the transmembrane domain of phospholamban (Adams *et al*., 1995). This analysis does not take into account the range of values reported for the amide I transition moment orientation. Helix tilt angles closer to $\theta = 23°$ would be obtained if the value used for the transition moment angle, α, were chosen to be closer to the 39–40° angle reported by Bradbury *et al*. (1962) and Tsuboi (1962) (see Materials and Methods).

Effect of phosphorylation on phospholamban structure and orientation

Phosphorylation of Ser16 and Thr17 is the mechanism for regulation of phospholamban function. ATR-FTIR spectra obtained from phosphorylated PLBWT are shown in Figure 4(a) and (b), and are similar to those obtained from PLBWT (in both secondary structure and dichroism, i.e. orientation). Order parameters calculated from these measurements (R^{ATR}max = 3.1, S_{helix} = 0.46) correspond to a helical tilt angle of 32.5 (± 4.5)°, indicating that no significant change in conformation takes place as a result of phosphorylation. Furthermore, the local secondary structure at the phosphorylation site

Table 2

ATR-FTIR dichroic ratios, order parameters and calculated tilt angles

Vibrational mode	PLBWT amide I 1656 cm^{-1}	PLBTM amide I 1656 cm^{-1}	Lipid CH_2 2924 cm^{-1}	Lipid CH_2 2852 cm^{-1}
$\langle R^{ATR} \rangle / R^{ATR}max$[a]	2.9/3.31	2.74/3.43	1.12/1.05	1.07/0.94
$\langle S \rangle / Smax$[b]	0.41/0.54	0.35/0.58	0.69/0.76	0.75/0.89
Tilt angle (θ)[c] (deg.)	30(±4)	27.5(±4.5)	27	24

[a] $\langle R^{ATR} \rangle$ is the average observed dichroic ratio from >6 independent measurements. $R^{ATR}max$ is the maximum dichroic ratio determined in the case of the protein amide I vibration, and the minimum dichroic ratio determined in the case of the lipid vibrations.

[b] $\langle S \rangle$ is the order parameter calculated from the average dichroic ratio $\langle R^{ATR} \rangle$. *S*max is the order parameter calculated from the maximum dichroic ratio determined in the case of the protein amide I vibration, and the minimum dichroic ratio determined in the case of the lipid vibrations.

[c] See the text for details on the tilt angle calculations.

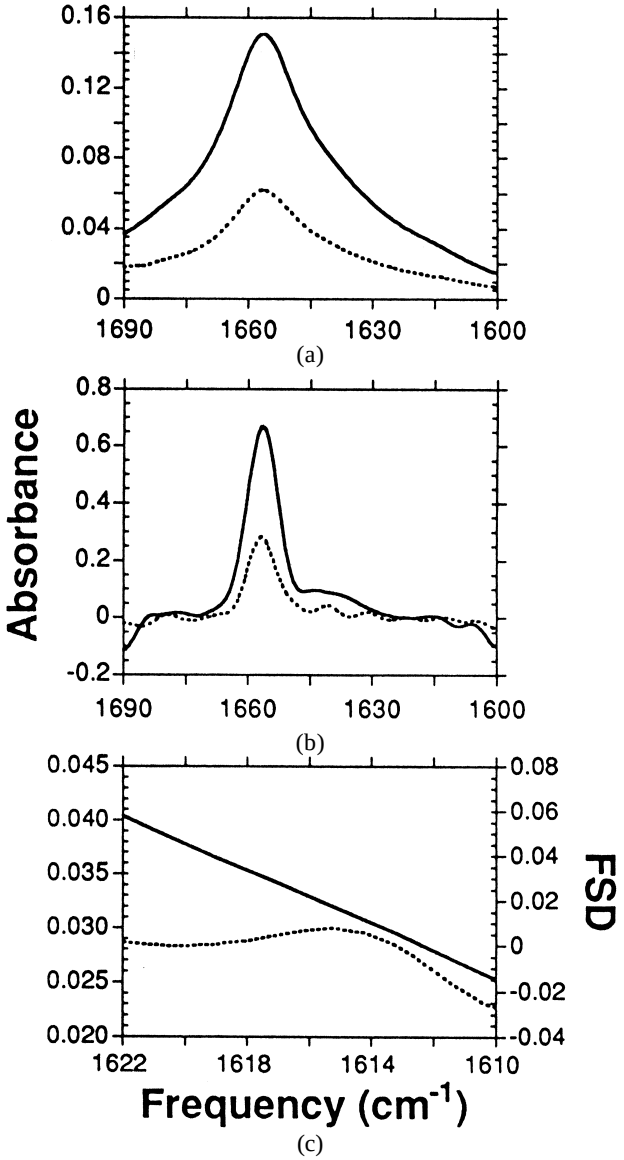

Figure 4. Polarized ATR-FTIR spectra (a) and Fourier self-deconvolutions (b) of PLBWT-P. Spectra were obtained with parallel (continuous line) or perpendicular polarized light (broken line). (c) An expansion of the parallel polarized ATR-FTIR spectrum in the region of the ^{13}C isotope-shifted amide I mode of PLBWT-P (continuous line) and the corresponding Fourier self-deconvolution (broken line).

(Ile12-Ser16) remains helical upon phosphorylation, as is evident from the ^{13}C isotope induced shift of the amide I mode of Ile12 (see above).

Structural model of phospholamban

Transmission FTIR and CD spectroscopic measurements of PLBTM and PLBWT clearly establish that both the cytosolic and transmembrane regions of the protein have predominantly α-helical

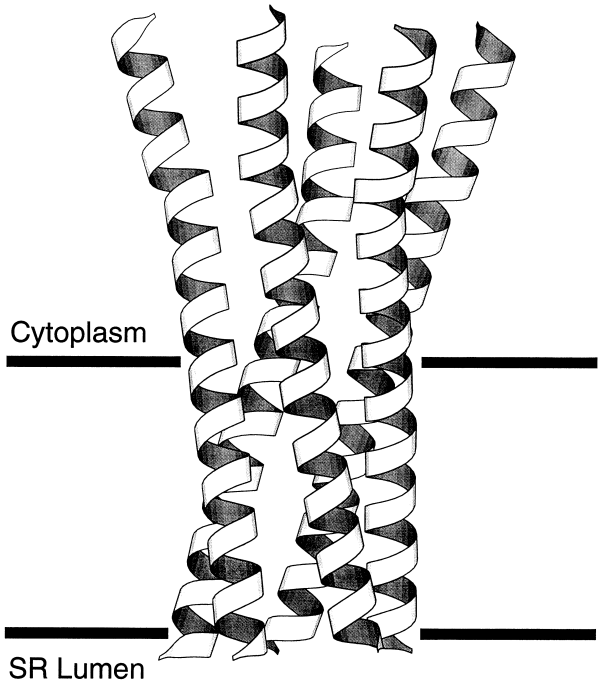

Figure 5. Model of the phospholamban ion channel complex. The CD and FTIR data indicate that the protein is highly helical and that the helix is oriented perpendicular to the membrane plane with a tilt angle of 28(±6)°. The complex is modeled based on the structure of the transmembrane domain previously proposed using computational methods (Adams *et al.*, 1995) and extending the transmembrane helices to Ile12. The helices pack tightly together in a highly specific manner as determined by site-directed mutagenesis (Arkin *et al*., 1994) and are thought to associate in a left-handed coiled-coil arrangement (Adams *et al*., 1995).

secondary structure. Furthermore, both the transmembrane and cytosolic α-helical elements share the same perpendicular orientation with respect to the membrane plane. Starting from the carboxy terminus, the roughly 22 residues determined by FTIR to be helical in PLBTM most likely span the bilayer as a transmembrane α-helix. The question now remains as to whether the cytosolic helical element (approx. 15 residues) is continuous with the transmembrane α-helix or, as suggested by Jones and co-workers (Simmerman *et al*., 1989), is separated by an unstructured stretch of amino acid residues. Several lines of evidence support the model of a continuous helix. First, the cytosolic segment, when separated from the transmembrane domain, is no longer α-helical in solution (Terzi *et al*., 1992), while the transmembrane domain (PLBTM) when synthesized on its own is largely helical. This implies that there may be helical nucleation by the transmembrane domain. Second, a rigid connecting region would be required for a discontinuous cytosolic helix to be highly oriented in a nearly identical fashion to the transmembrane helix. Finally, the CD thermal profile indicates that the entire helical content of the protein is extremely stable. This is typical of transmembrane α-helices but would not be expected for a disjointed soluble helix. The model predicts a channel structure whose pore extends above the membrane surface. Interestingly, the conductance of the transmembrane peptide (100 to 150 pS) is considerably higher than that of the full-length protein (10 to 20 pS: Kovacs *et al*., 1988; Arkin *et al*., 1993) suggesting that there is a restriction in the pore of the full-length protein that is absent in PLBTM. The fact that PLBTM, a peptide that completely lies within the proposed α-helical segment of PLBWT, is only 77% helical (as determined by FTIR) may imply that breaking the α-helix further unfolds it.

The model proposed for the complex (Figure 5) is a symmetrical bundle of five long helices (40 amino acid residues in length) stretching from the carboxy terminus of phospholamban. The helices pack tightly together in a highly specific manner as determined by mutagenesis (Arkin *et al*., 1994) and are thought to associate in a left-handed coiled-coil arrangement (Adams *et al*., 1995). A bend of 25° (Yun *et al*., 1991) has been introduced at the position of Pro21 (Barlow & Thornton, 1988). The helical bundle spans the bilayer and extends into the cytosol forming a long ion pore. The α-helical bundle extends toward the recognition and phosphorylation sequence of PLBWT, 17 to 29 Å into the cytoplasm (approx. 11 to 19 residues). A helical wheel projection at a pitch

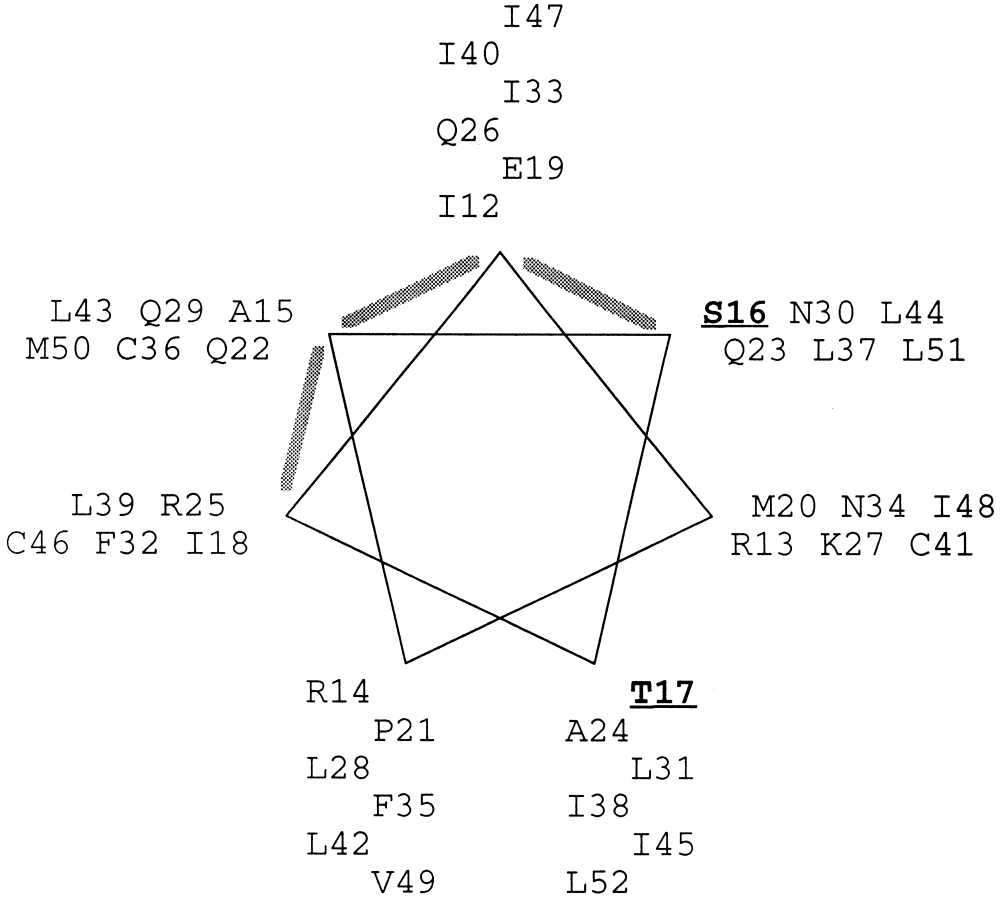

Figure 6. Helical wheel diagram of human phospholamban residues Ile12 to Leu52. The helix faces that are thought to interact and / or line the ion pore are shaded. The 2 residues (Ser16 and Thr17) that can be phosphorylated are in bold, underlined text.

corresponding to the interacting surfaces of a left-handed coiled-coil (3.5 amino acid residues/turn) of the residues presumed to be α-helical is shown in Figure 6. The interacting surfaces of the helices as well as the helix face lining the ion pore derived from site-directed mutagenesis (Arkin *et al*., 1994) and computational studies (Adams *et al*., 1995) are depicted. This model, as expected, positions both Ser16 and Thr17 on the surface of the complex. The remainder of the N-terminal amino acid residues of phospholamban may be non-helical.

Proposed mechanism for regulation of the Ca^{2+} ATPase by phospholamban

The prevailing hypothesis describing the mechanism of phospholamban's inhibitory effect on the Ca^{2+} ATPase is based upon an inhibitory complex between these two proteins that dissociates upon phospholamban phosphorylation (James *et al*., 1989). It is thought that the affinity of phospholamban for the Ca^{2+} ATPase is a function of the cytosolic segment of phospholamban since mutagenesis of amino acids Glu2 to Ile18, all residing in the cytosolic segment of phospholamban, reduced the inhibitory effect of phospholamban on the Ca^{2+} ATPase (Toyofuku *et al*., 1994). However, peptides corresponding to the cytosolic segment of phospholamban had no effect on the activity of Ca^{2+} ATPase (Jones & Field, 1993).

An additional property of phospholamban, Ca^{2+} selective conductance, suggested that phospholamban may inhibit the pump by acting as a pathway to equilibrate Ca^{2+} across both sides of the SR membrane, thereby negating the Ca^{2+} ATPase function (Kovacs *et al*., 1988). Such a suggestion would also imply that phosphorylation of phospholamban would abolish ion flow, although the effect of phosphorylation on phospholamban conductance has not been reported.

Based on time-resolved phosphorescence anisotropy, Thomas and co-workers (Voss *et al*., 1994) have recently found that phosphorylation of phospholamban increases the rotational mobility of Ca^{2+} ATPase in SR membranes. They observed the largest changes associated with Ca^{2+} ATPase molecules immobilized in large aggregates. On the basis of this data, they suggest that large scale aggregation of the phospholamban pentamer with ten or more Ca^{2+} ATPase molecules may be required for inhibition.

We suggest a mechanism in Figure 7 that incorporates all of the ideas above and is consistent with the observation that phosphorylation does not lead to a significant change in phospholamban structure or orientation. In this model the cytosolic domain of phospholamban in both its native and phosphorylated states restricts Ca^{2+} conductance relative to the transmembrane domain alone. Removal of the inhibitory cytosolic domain increases Ca^{2+} conductance by roughly an order of magnitude (Kovacs *et al*., 1988; Arkin *et al*., 1993). We suggest

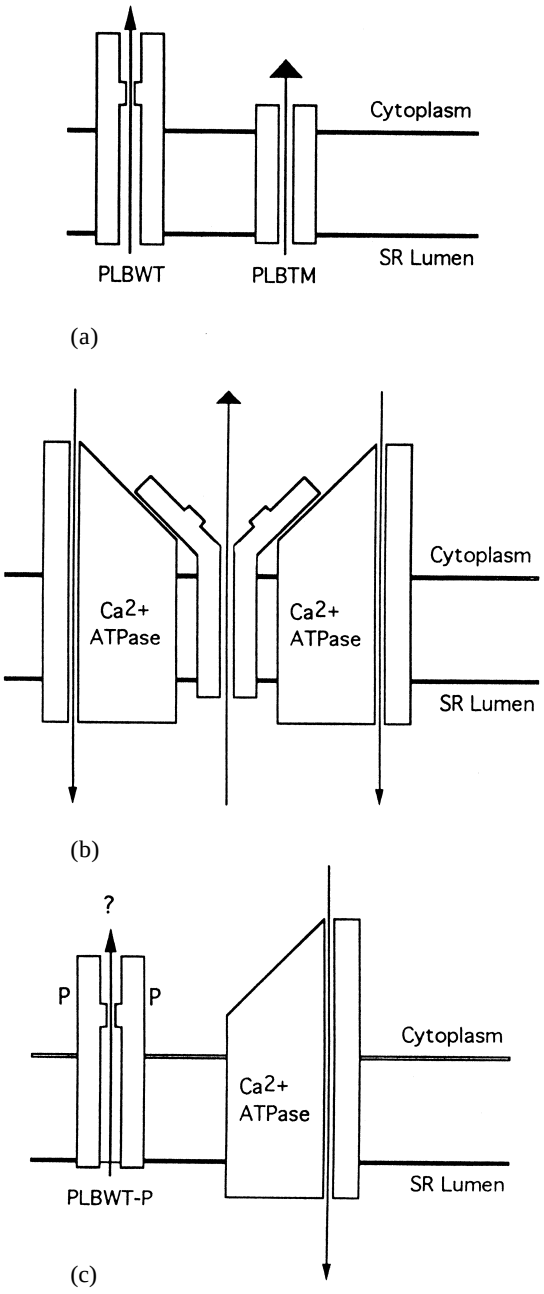

Figure 7. Schematic representation of a proposed mechanism for the regulation of Ca^{2+} levels across SR membranes by phospholamban. The arrows show the direction of Ca^{2+} flow. For simplicity only 2 out of the 5 members of the phospholamban pentameric complex are shown interacting with 2 Ca^{2+} ATPase molecules. (a) In the absence of the Ca^{2+} ATPase, the cytosolic segment of PLBWT restricts the flow of Ca^{2+} into the cytoplasm to 10 to 20 pS Kovacs *et al*., 1988). For comparison, the Ca^{2+} conductance of PLBTM is 100 to 150 pS (Kovacs *et al*., 1988; Arkin *et al*., 1993). (b) The cytoplasmic domain of PLBWT (unphosphorylated) interacts with the Ca^{2+} ATPase (James *et al*., 1989; Toyofuku *et al*., 1994). We propose that this interaction relieves the inhibitory effect of the cytosolic segment of PLBWT on Ca^{2+} conductance, thereby short circuiting the Ca^{2+} pump. (c) The complex between phospholamban and the Ca^{2+} ATPase dissociates upon phospholamban phosphorylation (James *et al*., 1989) and may reduce ion conductance by PLBWT.

regulation takes place through binding of phospholamban to the Ca^{2+} ATPase, resulting in a conformational change of the cytosolic domain of phospholamban that increases ion conductance. Phosphorylation, the regulatory switch, results in complex dissociation and reduction in phospholamban conductance. Studies are underway to determine the effect of Ca^{2+} ATPase and phosphorylation on phospholamban conductance.

Materials and Methods

Protein purification and reconstitution

PLBWT and PLBTM were synthesized using tert-butyl carbamate derivatives on a solid phase support, cleaved from the resin with hydrofluoric acid and lyophilized. The lyophilized peptides were dissolved in 1 ml of trifluoroacetic acid (final concentration approx. 4 mg / ml) and immediately injected onto a 5 ml POROS-R1 reverse phase high performance liquid chromatography (RP-HPLC) column (Perceptive Biosystems, Cambridge, MA) equilibrated with 95% H_2O, 2% (w / v) acetonitrile and 3% (v / v) 2-propanol. Peptide elution was achieved with a linear gradient to a final solvent composition of 5% H_2O, 38% acetonitrile and 57% 2-propanol. All solvents contained 0.1% (v / v) trifluoroacetic acid. Fractions containing peptides were then lyophilized and assessed for purity by amino acid analysis (correlation coefficients of >0.95) and mass spectrometry. The pure lyophilized peptides were dissolved with a solution of 20% (w / v) octyl β-glucoside (Sigma, St Louis, MO) to a final concentration of 4 mg / ml. A 500 µl solution containing 20 mg DMPC / ml (Avanti Polar Lipids, Alabaster, AL) and 10% octyl β-glucoside was added to the protein and reconstitution of the peptides into the phospholipids was achieved by exhaustive dialysis into a buffer containing 1 mM Tris-HCl (pH 7.4: Sigma, St Louis, MO). The lipid to protein ratios were ∼120:1 (PLBWT) and 80:1 (PLBTM).

CD spectroscopy

CD measurements were performed on an Aviv 62DS circular dichroism spectrometer (Lakewood, NJ) at 37°C using a 1 mm path-length cuvette (Helma, Jamaica, NY). The samples were diluted fivefold resulting in a final buffer concentration of 0.2 mM Tris-HCl (pH 7.4). Peptide concentrations (8 to 18 µM) were determined with replicate samples by amino acid analysis employing prolonged hydrolysis. For the CD thermal profile, the sample (60 µM) was not diluted and the wavelength was held at 222 nm.

Infrared spectroscopy

FTIR spectra were recorded on a Nicolet Magna 550 spectrometer purged with N_2 (Madison, WI) and equipped with a MCT / A detector. Interferograms (1000) recorded at a spectral resolution of 4 cm^{-1} were averaged for each sample. Interferograms were processed using one point zero filling and Happ-Genzel apodization, followed by automatic baseline correction. Peak integration was performed on Fourier self-deconvoluted spectra (Kauppinen *et al*., 1981), using a bandwidth of 13 cm^{-1} and an enhancement factor of 2.4, determined by Byler & Susi (1986) to best fit experimental data. For transmission spectra, 50 µl of sample (protein concentration of 36 to 90 µM) was dried on AgCl windows with dry air. For polarized ATR-FTIR spectra the spectrometer was equipped with a KRS-5 wire grid polarizer (0.25 µm spacing, Graseby Specac, Kent, UK). The sample (∼300 µl, 36 to 90 µM) was dried on the surface of a Ge internal reflection element (52 mm × 20 mm × 2 mm) and placed in a variable angle ATR accessory (Graseby Specac, Kent, UK).

Analysis of orientation from ATR-FTIR dichroism

The electric field amplitudes of the evanescent wave are given by Harrick (1967):

$$E_x = 2(\sin^2\phi - n_{21}^2)^{1/2}\cos\phi / [(1 - n_{21}^2)^{1/2}[(1 + n_{21}^2)\sin^2\phi - n_{21}^2]^{1/2}]$$

$$E_y = 2\cos\phi / (1 - n_{21}^2)^{1/2}$$

$$E_z = 2\sin\phi\cos\phi / [(1 - n_{21}^2)^{1/2}[(1 + n_{21}^2)\sin^2\phi - n_{21}^2]^{1/2}]$$

where ϕ is the angle of incidence between the infrared beam and the internal reflection element (45°), and n_{21} is the ratio between the refractive indices of the sample (n_2 = 1.43) and the internal reflection element (n_1 = 4.0: Wolfe & Zissis, 1978; Fringeli *et al*., 1989; Tamm & Tatulian, 1993). These equations are based on the assumption that the thickness of the deposited film (>20 µm) is much larger than the penetration depth (∼1 µm) of the evanescent wave (see Harrick, 1967). The electric field components together with the dichroic ratio (defined as the ratio between absorption of parallel ($A_\parallel$) and perpendicular ($A_\perp$) polarized light, $R^{ATR} \equiv A_\parallel / A_\perp$) are used to calculate an order parameter defined as:

$$S \equiv 3/2\langle\cos^2\theta\rangle - 1/2$$

with the following equation:

$$S = 2(E_x^2 - R^{ATR}E_y^2 + E_z^2) / [(3\cos^2\alpha - 1)(E_x^2 - R^{ATR}E_y^2 - 2E_z^2)]$$

where θ is the angle between the helix director and the normal of the internal reflection element, and α is the angle between the helix director and the transition dipole moment of the amide I vibrational mode. Values for α in the literature range from 29 to 40° (29 to 34°, Miyazawa & Blout, 1961; 40°, Bradbury *et al*., 1962; 39°, Tsuboi, 1962). For the calculations in this study, we have assumed an average value of 35°. It should be noted, however, that the higher estimates of α taken from the more recent reports result in higher order parameters and subsequent lower tilt angles (see below). Order parameters of 1.0 and –0.5 correspond to helical orientations parallel and perpendicular to the membrane normal, respectively. Lipid order parameters are obtained from the lipid methylene symmetric (2852 cm^{-1}) and asymmetric (2924 cm^{-1}) stretching modes using the same equation by setting α = 90°.

Protein phosphorylation

Protein phosphorylation was performed as described by Voss *et al*. (1994). Briefly, lyophilized peptides (see above) were resuspended in 200 µl of a solution containing 25% Thesit (Boehringer Mannheim, Indianapolis, IN) and diluted to a final reaction volume of 2 ml with a mixture of 2.5% Thesit, 50 mM Tris-HCl (pH 7.0), 2 mM $MgCl_2$, 0.75 mM dATP (Boehringer Mannheim, Indianapolis, IN), 1 mM Tris-(2-carboxyethyl)phosphine hydrochloride (Pierce, Rockford, IL) and 2500 units of the catalytic

subunit of protein kinase A (Sigma, St Louis, MO). The reaction was performed for 8 hours at 30°C. The phosphorylation mixture was then re-loaded onto the RP-HPLC column and the protein was purified as described above. Peptide contained in appropriate HPLC fractions was lyophilized and reconstituted into DMPC vesicles. Phosphorylation levels were quantified from ^{32}P phosphorylation of a known concentration of phospholamban (amino acid analysis) followed by trichloroacetic acid precipitation. The protein was then resuspended in standard SDS protein sample buffer. Unreacted nucleotide was removed using centrifugal filtration followed by scintillation counting to determine the amount of phosphorylated protein. Minimum phosphorylation levels assuming 100% efficiency for trichloroacetic acid precipitation, resuspension and no loss during filtration, were calculated to be 74%.

Acknowledgements

We thank Dr Paul D. Adams for many helpful discussions and for preparing Figure 5. We also thank Dr David Stern for help with the quantitative phosphorylation experiments, and Dr James Elliott and Myron Crawford for their technical support for amino acid analyses and the synthesis of PLBWT. This work was supported by grants from the National Institutes of Health to S.O.S. (GM 46732), D.M.E. (GM 22778) and K.J.R. (6M 47527), and the U.S. Army Research Office to K.J.R. (DAALO3-92-G-0172).

References

Adams, P. D., Arkin, I. T., Engelman, D. M. & Brünger, A. T. (1995). Computational searching and mutagenesis suggest a structure for the pentameric transmembrane domain of phospholamban. *Nature Struct. Biol*. **2**, 154–159.

Arkin, I. T., Moczydlowski, E. G., Aimoto, S., Smith, S. O. & Engelman, D. M. (1993). Functional and structural studies of phospholamban as a model ion channel. *Biophys. J.* **64**, A207.

Arkin, I. T., Adams, P. D., MacKenzie, K. R., Lemmon, M. A., Brünger, A. T. & Engelman, D. M. (1994). Structural organization of the pentameric transmembrane α-helices of phospholamban, a cardiac ion channel. *EMBO J.* **13**, 4757–4764.

Bandekar, J. & Krimm, S. (1979). Vibrational analysis of peptides, polypeptides, and proteins: characteristic amide bands of β-turns. *Proc. Natl Acad. Sci., U.S.A.* **76**, 774–777.

Barlow, D. J. & Thorton, J. M. (1988). Helix geometry in proteins. *J. Mol. Biol.* **201**, 601–619.

Bradbury, E. M., Brown, L., Downie, A. R., Elliott, A., Fraser, R. D. B. & Hanby, W. E. (1962). The structure of the ω-form of poly-β-benzyl-L-aspartate. *J. Mol. Biol.* **5**, 230–247.

Braiman, M. S. & Rothschild, K. J. (1988). Fourier transform infrared techniques for probing membrane protein structure. *Annu. Rev. Biophys. Biophys. Chem.* **17**, 541–570.

Byler, M. D. & Susi, H. (1986). Examination of the secondary structure of proteins by deconvolved FTIR spectra. *Biopolymers,* **25**, 469–487.

Catterall, W. A. (1991). Functional subunit structure of voltage-gated calcium channels. *Science,* **253**, 1499–1500.

Chen, Y., Yang, J. T. & Chau, K. H. (1974). Determination of the helix and β form of proteins in aqueous solution by circular dichroism. *Biochemistry,* **13**, 3350–3359.

Duysens, L. N. M. (1956). The flattening of the absorption spectrum of suspensions as compared to that of solutions. *Biochim. Biophys. Acta,* **19**, 1–12.

Fringeli, U. P., Apell, H. J., Fringeli, M. & Lauger, P. (1989). Polarized infrared absorption of Na^+/K^+-ATPase studied by attenuated total reflection spectroscopy. *Biochim. Biophys. Acta,* **984**, 301–312.

Gasser, J. T., Chiesi, M. P. & Carafoli, E. (1986). Concerted phosphorylation of the 26 kDa phospholamban oligomer and of the low molecular weight phospholamban subunit. *Biochemistry,* **25**, 7615–7623.

Harrick, N. J. (1967). *Internal Reflection Spectroscopy*. Interscience Publishers, New York.

Hauser, H., Pascher, I., Pearson, R. H. & Sundell, S. (1981). Preferred conformation and molecular packing of phosphatidylethanolamine and phosphatidylcholine. *Biochim. Biophys. Acta,* **650**, 21–51.

James, P., Inui, M., Tada, M., Chiesi, M. & Carafoli, E. (1989). Nature and site of phospholamban regulation of the Ca^{2+} pump of sarcoplasmic reticulum. *Nature (London),* **342**, 90–92.

Jones, L. R. & Field, L. J. (1993). Residues 2-25 of phospholamban are insufficient to inhibit Ca^{2+} transport ATPase of cardiac sarcoplasmic reticulum. *J. Biol. Chem.* **268**, 11486–11488.

Kauppinen, J. K., Moffatt, D. J., Mantsch, H. H. & Cameron, D. G. (1981). Fourier self-deconvolution: a method for resolving intrinsically overlapped bands. *Appl. Spectrosc.* **35**, 271–276.

Kovacs, R. J., Nelson, M. T., Simmerman, H. K. B. & Jones, L. R. (1988). Phospholamban forms Ca^{2+} -selective channels in lipid bilayers. *J. Biol. Chem.* **263**, 18364–18368.

Long, M. M. & Urry, D. W. (1981). Absorption and circular dichroism spectroscopies. In *Membrane Spectroscopy* (Grell, E., ed.), vol. 31, pp. 143–171, Springer-Verlag, Berlin.

Mao, D. & Wallace, B. A. (1984). Differential light scattering and absorption flattening optical effects are minimal in the circular dichroism spectra of small unilamellar vesicles. *Biochemistry,* **23**, 2667–2673.

Miyazawa, T. & Blout, E. R. (1961). The infrared spectra of polypeptides in various conformations: amide I and amide II bands. *J. Amer. Chem. Soc.* **83**, 712–719.

Park, K., Perczel, A. & Fasman, G. D. (1992). Differentiation between transmembrane helices and peripheral helices by the deconvolution of circular dichroism spectra of membrane proteins. *Protein Sci.* **1**, 1032–1049.

Simmerman, H. K. B., Lovelace, D. E. & Jones, L. R. (1989). Secondary structure of detergent-solubilized phospholamban, a phosphorylatable oligomeric protein of cardiac sarcoplasmic reticulum. *Biochim. Biophys. Acta,* **997**, 322–329.

Smith, S. O., Jonas, R., Braiman, M. S. & Bormann, B. J. (1994). Structure and orientation of the transmembrane domain of glycophorin a in lipid bilayers. *Biochemistry,* **33**, 633–641.

Susi, H., Timasheff, S. N. & Stevens, L. (1967). Infrared spectra and protein conformations in aqueous solutions. I. The amide I band in H_2O and D_2O solutions. *J. Biol. Chem.* **243**, 5460–5466.

Tada, M. (1992). Molecular structure and function of phospholamban in regulating the calcium pump from

sarcoplasmic reticulum. *Ann. N.Y. Acad. Sci.* **671**, 92–102.

Tada, M. & Kadoma, M. (1989). Regulation of the Ca^{2+} pump ATPase by CAMP-dependent phosphorylation of phospholamban. *BioEssays,* **10**, 157–163.

Tada, M., Kadoma, M., Fujii, J., Kimura, Y. & Kijima, Y. (1989). Molecular structure and function of phospholamban: the regulatory protein of the calcium pump in cardiac sarcoplasmic reticulum. *Advan. Expt. Med. Biol.* **255**, 79–89.

Tadesse, L., Nazarbaghi, R. & Walters, L. (1991). Isotopically enhanced infrared spectroscopy: a novel method for examining secondary structure at specific sites in conformationally heterogeneous peptides. *J. Amer. Chem. Soc.* **113**, 7036–7037.

Tamm, L. K. & Tatulian, S. A. (1993). Orientation of functional and nonfunctional PTS permease signal sequences in lipid bilayers. A polarized attenuated total reflection infrared study. *Biochemistry,* **32**, 7720–7726.

Terzi, E., Poteur, L. & Trifillieff, E. (1992). Evidence for a phosphorylation-induced conformational change in phospholamban cytoplasmic domain by CD analysis. *FEBS Letters,* **309**, 413–416.

Tinoco, I., Woody, R. W. & Bradley, D. F. (1963). Absorption and rotation of light by helical polymers: the effect of chain lengths. *J. Chem. Phys.* **38**, 1317–1325.

Toyofuku, T., Kurzydlowski, K., Tada, M. & MacLennan, D. H. (1994). Amino acids Glu2 to Ile18 in the cytoplasmic domain of phospholamban are essential for functional association with the $Ca^{(2+)}$-ATPase of sarcoplasmic reticulum. *J. Biol. Chem.* **269**, 3088–3094.

Tsuboi, M. (1962). Infrared dichroism and molecular conformation of α-form poly-g-benzyl-l-glutamate. *J. Polymer. Sci.* **59**, 139–153.

Unwin, N. (1993). Nicotinic acetylcholine receptor at 9 Å resolution. *J. Mol. Biol.* **229**, 1101–1124.

Venyaminov, S. U. & Kalnin, N. N. (1990*a*). Quantitative IR spectrophotometry of peptide compounds in water (H_2O) solutions. I. Spectral parameters of amino acid residue absorption bands. *Biopolymers,* **30**, 1243–1257.

Venyaminov, S. U. & Kalnin, N. N.(1990*b*). Quantitative IR spectrophotometry of peptide compounds in water (H_2O) solutions. II. Amide absorption bands of polypeptides and fibrous proteins in alpha-, beta-, and random coil conformations. *Biopolymers,* **30**, 1259–1271.

Venyaminov, S. U. & Kalnin, N. N. (1990*c*). Quantitative IR spectrophotometry of peptide compounds in water (H_2O) solutions. III. Estimation of the protein secondary structure. *Biopolymers,* **30**, 1273–1280.

Voss, J., Jones, L. R. & Thomas, D. D. (1994). The physical mechanism of calcium pump regulation in the heart. *Biophys. J.* **67**, 190–196.

Wegener, A. D. & Jones, L. R. (1984). Phosphorylation-induced mobility shift in phospholamban in SDS-polyacrylamide gels. Evidence for a protein structure consisting of multiple identical phosphorylatable subunits. *J. Biol. Chem.* **259**, 1834–1841.

Wegener, A. D., Simmerman, H. K. B., Lindemann, J. P. & Jones, L. R. (1989). Phospholamban phosphorylation in intact ventricles. *J. Biol. Chem.* **264**, 11468–11474.

Wolfe, W. F. & Zissis, G. J. (1978). p. 1600, In *The Infrared Handbook,* U.S. Government Printing Office, Washington.

Yun, R. H., Anderson, A. & Hermans, J. (1991). Proline in α-helix: stability and conformation studied by dynamics simulation. *Proteins: Struct. Funct. Genet.* **10**, 219–228.

Edited by F. Cohen

(Received 4 November 1994; accepted in revised form 9 February 1995)